Characterization of Quasi-Single-Helicity States in a Low-Aspect-Ratio RFP

Kensuke OKI, Daisuke FUKAHORI, Kazuaki DEGUCHI, Seiya NAKAKI, Akio SANPEI, Haruhiko HIMURA, Sadao MASAMUNE and Roberto PACCAGNELLA[1)]

Kyoto Institute of Technology, Kyoto 606-8585, Japan

[1)]*Consorzio RFX and Istituto Gas Ionizzati del C.N.R, Padova, 35127, Italy*

(Received 5 January 2012 / Accepted 26 February 2012)

Characteristics of quasi-single-helicity (QSH) states have been studied in a low-aspect-ratio reversed field pinch (RFP) machine RELAX mainly by magnetic diagnostics. Internal profiles of the fluctuating radial, poloidal and toroidal magnetic fields have shown good agreement with eigenfunctions of a single helical mode. The edge magnetic fluctuation spectra are somewhat broader than what are expected from internal magnetic field profiles. In spite of these slight discrepancies, the usual measure for the QSH, the spectral index N_S lower than 2, still provides a reasonable measure for QSH states in RELAX. The QSH persistence has been improved in RELAX by the reduction of the poloidal resistance of flanges at poloidal gaps, mainly due to the improved axisymmetry of the toroidal magnetic field. QSH persistence more than 30% of the flat-topped current phase has been realized with current density lower than in other RFP, and probability of spontaneous QSH is $12.8 \pm 7.3\%$ which is higher than high-aspect-ratio RFP. It suggests the advantage of low-aspect-ratio configuration in attaining to the QSH. Comparison with recent experiments using active resonant perturbation may suggest the importance of further reduction of field errors to improve the quality of QSH.

Keywords: quasi-single-helicity (QSH), reversed field pinch, low aspect ratio RFP, magnetic fluctuation, internal magnetic field

DOI: 10.1585/pfr.7.1402028

1. Introduction

Reversed field pinch (RFP) is one of the toroidal magnetic confinement systems for compact, high-beta plasmas for nuclear fusion reactors. One of the characteristic features of the RFP is that it could confine high pressure plasmas with weak external magnetic field, and it has a potential for Ohmic ignition because there is no toroidal current limit in the RFP as the Kruskal-Shafranov limit in tokamaks. As a result, the safety factor of RFP is much less than 1 and hence $m = 1$ (m is poloidal mode number) tearing modes are dominant in the RFP.

Recent progress has led to new concepts for the RFP configurations which are free from magnetic chaos caused by the interaction of $m = 1$ tearing modes. One is the quasi-single-helicity (QSH) state where $m = 1$ with single n (n is toroidal mode number) mode grows to dominate a discharge [1]. In QSH, a large helical magnetic island associated with the innermost resonant mode is formed and (electron) confinement is improved inside the island. This leads to helical deformation of axisymmetric RFP configuration without control using external helical coils. More recently, single helical axis (SHAx) state, where the original axisymmetric magnetic axis disappears as the dominant island grows, has been founded in RFX-mod [2]. The SHAx state is theoretically predicted to be more resilient to magnetic chaos [3]. From the viewpoint of fusion plasmas, QSH is one of the candidates for improved confinement states for RFP.

The aspect ratio A ($= R_0/a =$ (major radius)/(minor radius)) is one of the remaining parameters for geometrical optimization of the RFP configuration. Recent theoretical works have shown that the resonant surfaces for the $m = 1$ modes become less densely spaced in the core region as the aspect ratio is lowered [4]. This leads to avoidance of overlap of magnetic islands and may allow us to expect easier access to the QSH state. RELAX is a low-A RFP machine to explore the characteristics of low-A RFP configurations. Initial results from RELAX on QSH have been reported particularly with emphasis on imaging diagnostics [5–8]. In this paper, major characteristics of QSH in RELAX (i.e., low-A RFP) is discussed based on major magnetic diagnostics results.

2. Experimental Apparatus

Figure 1 shows a top view of the RELAX machine with arrangement of magnetic diagnostics. In RELAX, we have used a 4-mm thick SS vacuum vessel with major radius R_0 of 508 mm and minor radius a of 250 mm, thus the aspect ratio A is as low as 2 [9]. The vessel has two poloidal gaps. Most experiments reported here were carried out with a single insulated gap; one of the gaps was

author's e-mail: ohki6t@nuclear.es.kit.ac.jp; masamune@kit.ac.jp

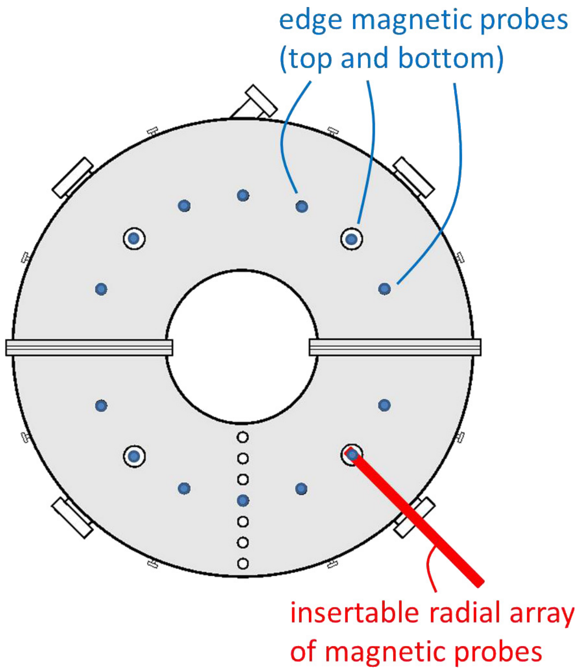

Fig. 1 Top view of RELAX with arrangement of magnetic diagnostics.

electrically insulated with a 10-mm wide Teflon flange, and the other, electrically connected with a SS flange. In the later part of this paper, we will discuss the improvement of toroidal symmetry of the toroidal magnetic field. These experiments were carried out with two insulated gaps with the modified SS flanges of the vacuum vessel; by increasing the poloidal resistance of the 4 flanges at the gaps, the resultant L/R time constant of the flanges at one gap (width = 50 mm) was decreased from 1.7 ms to 0.92 ms (~0.19 ms at the wall except the gaps having corresponding width). Since the toroidal field coil current starts to be reversed in coincidence with the start of plasma current and toroidal flux slightly vary during the discharge, the reduced time constant has the effect of realizing improved axisymmetry of the toroidal field. We should note that the $m = 1$ vertical and horizontal field errors were compensated for using 4 saddle coils with feedback controlled currents at each insulated gap.

In RELAX, edge magnetic probes are installed at the top and bottom ports at 14 toroidal locations equally spaced except at the two gaps. Toroidal separation angle is 22.5 degree, and there are no probes at the locations of the two gaps. The difference in the signals from the top and bottom coils provides odd m (mostly $m = 1$) modes, while the summation, the even m (mostly $m = 0$) modes. For the fluctuation analyses, these signals were numerically filtered, then spatially Fourier transformed to provide the amplitudes and phases of the modes with toroidal mode number (n) up to 8.

An insertable radial array of magnetic probes is installed at a port on the equatorial plane. The radial array is inserted from outboard side. The array consists of 8 magnetic probes separated by 36 mm. We can measure the radial field B_r, poloidal field B_θ and toroidal field B_ϕ at 8 radial locations from the geometric center of the vessel out to the inner surface of the vessel.

Cross-sectional average of the toroidal magnetic field is measured with a toroidal flux loop on the outer surface of the vacuum vessel. 16 flux loops approximately equally spaced in the toroidal direction form a toroidal array. The average toroidal field $\langle B_\phi \rangle$ is defined as the toroidally averaged values from 12 of these 16 flux loops except near the gaps.

In addition to the above magnetic diagnostics, we have soft-X ray diagnostics for emissivity profile measurement or estimates from tangential and vertical ports.

In what follows, we will discuss some of the characteristics of the QSH states in RELAX plasmas mainly from magnetic measurements. The QSH is a state where a single (usually core resonant tearing) mode dominates a discharge with lower-amplitude neighboring modes or the secondary modes. The spectral index N_S defined as follows is often used as a measure of the QSH,

$$N_S = \left[\sum_{n=4}^{8} \left(\frac{(b^{1,n})^2}{\sum_{n=4}^{8} (b^{1,n})^2} \right)^2 \right]^{-1} \tag{1}$$

where $b^{1,n}$ is the amplitude of the $m = 1$ mode with toroidal mode number n. The amplitude of each mode is obtained by spatial Fourier transformation of 2-50 kHz filtered edge toroidal magnetic fields. Sum of the amplitudes in the definition of N_S (Eq. (1)) is taken over the internally resonant $m = 1$, $n = 4$-8 modes. We should note that the upper bound of the toroidal mode number of 8 is a result of restriction by the number of pickup coils in our present toroidal array. The innermost resonant surface is believed to be for the $m = 1/n = 4$ mode ($q = 0.25$) from the equilibrium reconstruction [10–12].

$N_S = 1$ if a single mode dominates the edge magnetic fluctuation, while in the other extreme case where all the modes have the same amplitudes, N_S equals the number of resonant modes taken into account in the analysis (summation in Eq. (1)). It is a convention that the QSH is realized when $N_S < 2$, where in the case of $N_S = 2$ the dominant mode amplitude equals the sum of amplitudes of the remaining secondary modes.

3. Results

3.1 QSH discharge in RELAX

Figure 2 shows typical waveform of the QSH discharge in RELAX. Here $B_\phi(a)$ is the edge toroidal field averaged over all the edge magnetic probes at top and bottom ports. The field reversal parameter F ($\equiv B_\phi(a)/\langle B_\phi \rangle$) and the pinch parameter Θ ($\equiv B_\theta(a)/\langle B_\phi \rangle$, $B_\theta(a)$ is poloidally averaged edge poloidal magnetic field) are often used to describe a rough idea about RFP equilibrium. In the case of Fig. 2, the discharge with shallow reversal (or weakly

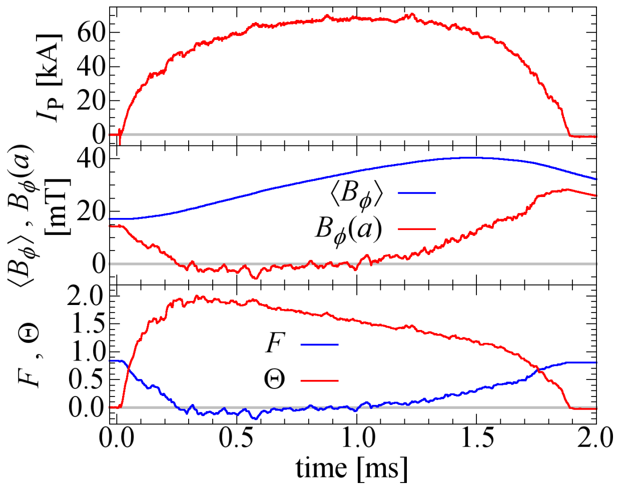

Fig. 2 Time evolution of the plasma current I_P, average toroidal magnetic field $\langle B_\phi \rangle$, averaged edge toroidal magnetic field $B_\phi(a)$, field reversal parameter F, and pinch parameter Θ in a typical QSH discharge in RELAX.

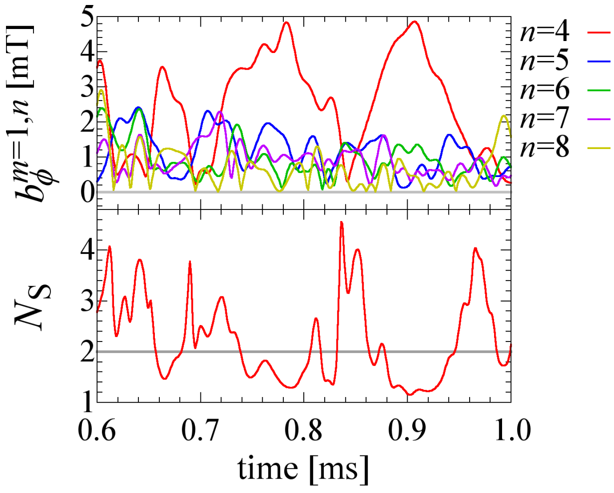

Fig. 3 Quasi-periodic oscillation of a single dominant $m = 1/n = 4$ mode and associated change in spectral index N_S in the flat-topped current phase.

reversed) RFP plasma is realized from 0.25 ms to 1.1 ms, then non-reversal, small positive F state is maintained to the end of the discharge.

QSH in RELAX tends to appear more frequently in relatively shallow reversal ($-0.3 < F < 0$) or weakly non-reversal ($0 < F < 0.3$) regions. Since Θ has correlation with F, Θ lies in the range $1.4 < \Theta < 1.8$ for these QSH regimes. Hereafter we will use F to specify the RFP state. The toroidal mode spectrum of the odd m (mostly $m = 1$) modes time-averaged over the flat-topped current phase has peaked profile around the core resonant modes, $n = 4$-6 [12]. The QSH state defined by $N_S < 2$ appears quasi-periodically in the flat-topped current phase with dominant mode of $n = 4$ in RELAX [13]. The dominant toroidal mode number of 4 arises from the low-A nature of RELAX, because the innermost resonant surface is believed to be for the $m = 1/n = 4$ mode.

Figure 3 shows an example of the appearance of QSH in RELAX. During a certain period of time, only the single $m = 1/n = 4$ mode grows to dominate the edge magnetic fluctuation, with lower amplitudes of the secondary modes. The QSH state lasts for a certain period of time, then back-transition to multi-helicity (MH) state occurs. The toroidal mode spectrum averaged over the time period during the QSH phase has a sharp peak at $n = 4$, as expected [13]. Hereafter the time period during which $N_S < 2$ will be referred to as QSH duration, and the fraction of the sum of the duration of QSH events in the flat-topped current phase will be referred to as the QSH persistence or QSH fraction.

3.2 Internal magnetic field profiles in QSH

In QSH discharges of RELAX, internal magnetic fields measured by a radial array of magnetic probes oscillate largely at about 10 kHz and the amplitude profiles are good agreement with the theoretical helical symmetric Ohmic equilibrium of cylindrical plasma [14]. A comparison of the experimental profiles at a time measured in $0.6 < r/a < 1.0$ (r is minor radial coordinate) by a radial array from top port and theoretical profiles has been shown in [14]. In what follows, we show the result measured in $-0.06 < r/a < 1.0$ by the radial array from an outboard port on the equatorial plane and more systematical comparison of the experimental and theoretical profiles.

Figures 4 and 5 are time evolution of magnetic fields and oscillating (2-50 kHz) component b of the magnetic fields measured at $-0.06 < (R - R_0)/a < 1.00$ (R is major radial coordinate) by the radial array. These oscillations at $\sim$10 kHz suggest rotation of a QSH helical state. This frequency is about constant in a flat-toped current phase from 0.5 to 1.5 ms, so phase velocity in toroidal direction is considered to be also about constant. The radial component of the magnetic field is $\pi/2$ out of phase in the oscillation from the poloidal and toroidal components. Dots in Fig. 6 show radial profiles of the three components of the magnetic field measured with the radial array. The profiles for low-frequency (< 2 kHz) or equilibrium component are in Fig. 6 (a), and those for the fluctuating component (2-50 kHz), dominantly at $\sim$10 kHz, in Fig. 6 (b). All quantities are time-averaged values during a flat-topped current phase from 0.5 to 1.5 ms in each discharge, and ensemble-averaged over 5 identical discharges. The radial profiles of the slowly varying components look similar to the Bessel function profiles, but slightly modified by the Shafranov shift of about 20% of the minor radius. Note that the fluctuating components in Fig. 6 (b) show the amplitudes with phase information; the fluctuating magnetic fields are multiplied by sign (+1 or −1) of a reference magnetic field at each time and averaged over the time. The reference for b_r is b_r measured at $(R - R_0)/a \sim 0.51$, and that for b_θ and b_ϕ

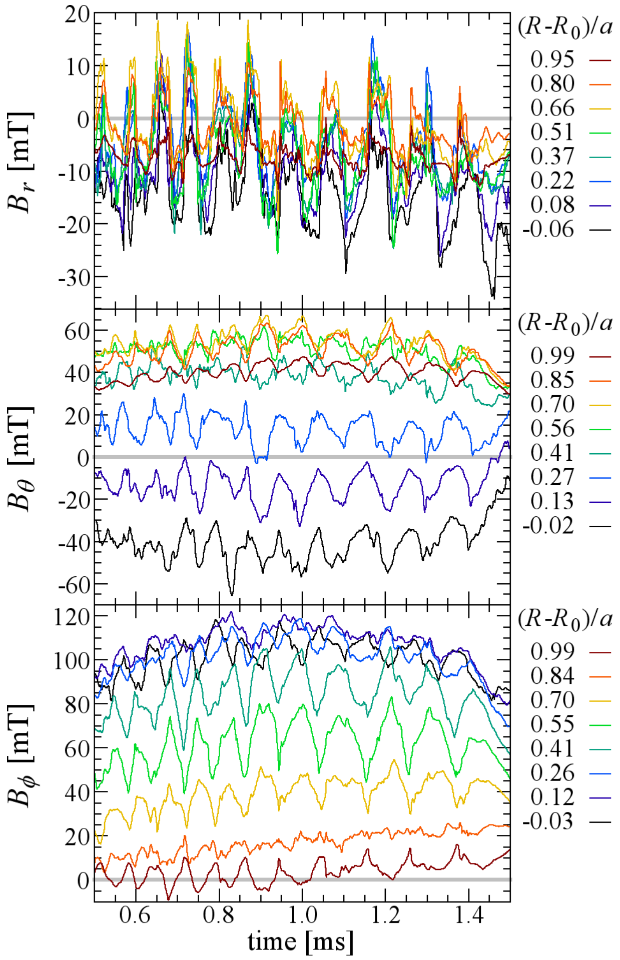

Fig. 4 Time evolution of magnetic fields measured by the radial array.

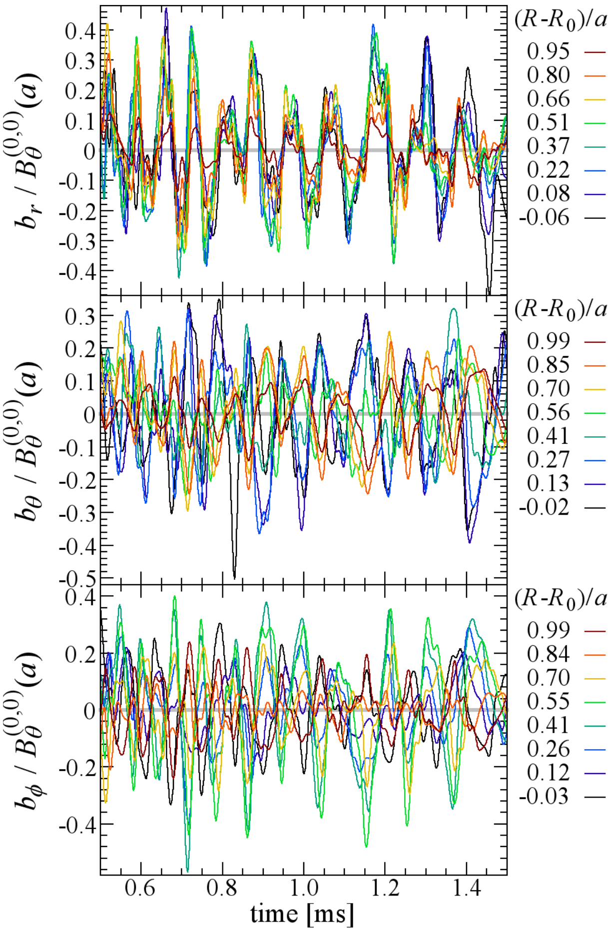

Fig. 5 Time evolution of oscillating (2-50 kHz) component b of magnetic fields measured by the radial array, which is normalized by the non-oscillating (< 2 kHz) component of an edge poloidal magnetic field $B_\theta^{(0,0)}(a)$.

is b_ϕ at $(R-R_0)/a \sim 0.55$. These time-averaged amplitudes are also multiplied by $\pi/2$ because sin wave averaged over the half period is $2/\pi$ per unit amplitude.

The solid lines are obtained from the helical Ohmic equilibrium model with cylindrical approximation [15,16]. The helical Ohmic equilibrium state is the simultaneous solution of the helically symmetric Grad-Shafranov equation and generalized Ohm's law with helical symmetry. The solution can be separated into axisymmetric and helically symmetric components. The solid lines in Fig. 6 (a) are for the axisymmetric part, and those in Fig. 6 (b) for the helically symmetric part. In the comparison in Fig. 6, the cylinder center ($r = 0$) of the theoretical profile is chosen at $(R - R_0)/a = 0.2$ and the cylinder radius a as $(R - R_0)/a = 0.8$ to take into account the experimental Shaflanov shift. These averaged experimental profiles agree well with the theoretical profiles and the standard deviations (error bars) are low. Thus, rotating helical state is suggested by the internal magnetic measurement.

3.3 Improved QSH fraction

One of the recent findings is that the QSH fraction (persistence), defined by the fraction of the total time periods in which $N_S < 2$ in the flat-topped current phase, has increased or improved by the modification of the flanges at the poloidal gaps. The modification has been made for the purpose of increasing the poloidal resistance of the flanges. As described in the previous section, the resultant reduction of the L/R time constant of the flanges has resulted mainly in improved toroidal symmetry or error fields. In Fig. 7, we have compared the QSH persistence (fraction) from 0.6 to 1.1 ms, corresponding to the flat-topped current phase, before and after the modification of the flanges. The large number of experimental points at $I_P \sim 55$ kA and 65-70 kA reflects the fact that most experiments were carried out at these values of flat-topped toroidal plasma current. It is clear that the QSH persistence (fraction) has increased from less than 20% to more than 30%. There seems to be no significant dependence of the QSH persistence (fraction) on the plasma current I_P or F.

Figure 8 shows the relation between QSH duration

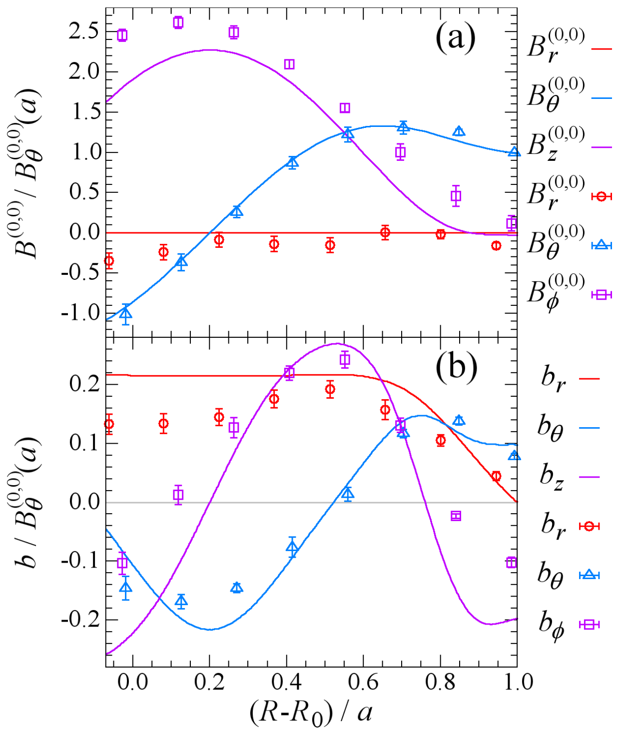

Fig. 6 Comparison of radial profiles of magnetic fields of experiment (dots) and the theoretical helical Ohmic equilibrium (lines). (a) is the experimental non-oscillating (< 2 kHz) component averaged over the flat-topped phase in 5 discharges and the theoretical poloidally and toroidally symmetric component. (b) is the experimental time averaged amplitude of oscillating (2-50 kHz) component averaged over the 5 discharges and the theoretical helical component.

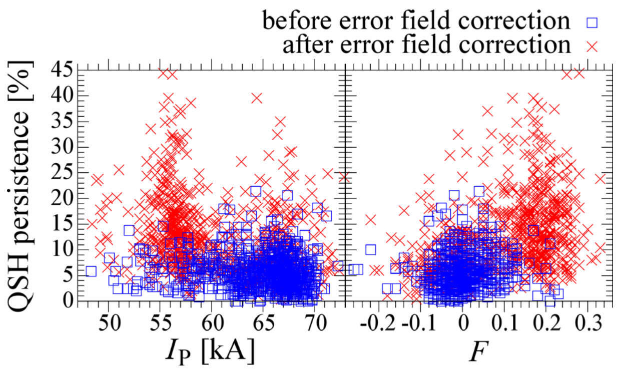

Fig. 7 QSH fraction (persistence) in the flat-toped current phase vs. plasma current I_P and F before and after the error field correction by the poloidal flange modification. The data set consists of results from more than 1000 shots.

and the mode amplitude (normalized to the poloidally averaged edge poloidal field) for $m/n = 1/4$, 1/5, and 1/6 modes averaged over the duration. At short QSH duration (< 0.02 ms), dominant mode is sometimes $n = 5$ or 6, which are not believed to be innermost resonant. But as the QSH duration is longer, probability that dominant

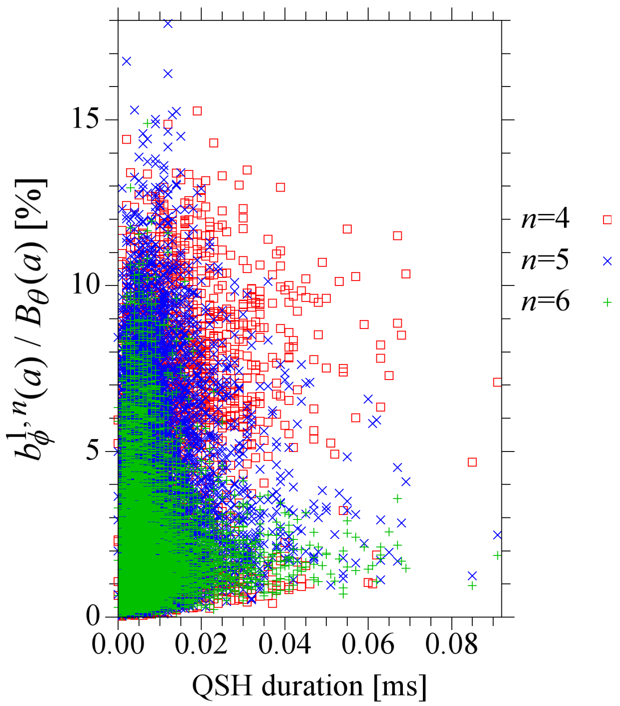

Fig. 8 QSH duration in the flat-topped current phase vs. amplitude of $m = 1$ and possible internally resonant n modes of the edge toroidal field fluctuation averaged over the duration.

mode is innermost $n = 4$ is higher, and at long QSH duration (> 0.04 ms), dominant mode is mostly $n = 4$. Because the innermost resonant mode contributes to confinement improvement in the core, the long QSH duration is more desirable. The non-innermost resonant dominant mode at the short QSH duration may be caused partly by the error fields.

Average of the QSH persistence over all shots after the error field correction in Fig. 7 (total 634 shots), which corresponds to probability of QSH (without external active control) in RELAX, is 12.8 ± 7.3%. This value is larger than probability of spontaneous QSH in high-aspect-ratio ($A = 6.8$) EXTRAP T2R device which is < 3% [17]. This fact suggests advantage of low-A configuration in attaining to the QSH as expected from the theoretical works.

4. Discussion

Easy access to QSH in shallow reversal regions agrees with a model recently proposed by Bonfiglio *et al.* [18]. In RELAX, even in the weakly non-reversal region ($0 < F < 0.3$), discharge parameters such as plasma current, loop voltage, and flat-toped current duration are similar to shallow reversal cases, and QSH state is also observed as shown in Fig. 7. Note that F in RELAX is evaluated from the average over the edge toroidal magnetic fields measured at top and bottom ports and toroidal effect is very large due to low aspect ratio. Thus, even when $F > 0$, the reversal or non-reversal of an edge toroidal magnetic field depends on time and poloidal and toroidal position due to the large fluctuation (oscillation) level $b_\phi(a)/B_\theta(a) \sim$ 5-10% (at ~10 kHz).

Relatively short duration of QSH (tens of μs) compared with the flat-toped current phase may be partly determined by resistive diffusion time [17]. The resistive diffusion time in RELAX is roughly estimated to be < 0.1 ms. QSH persistence has been increased by the modification of the poloidal flanges as shown in Fig. 7, and the innermost $n = 4$ mode is more dominant in $m = 1$ modes at longer QSH duration phases as shown in Fig. 8. Thus, the short duration of QSH or quasi-periodic appearance (or disappearance) of QSH and non-innermost resonant dominant mode may be partly caused by error fields due to flanges; the field errors may disturb QSH measurement by the edge magnetic probes and purer QSH itself.

The internal magnetic field profiles measured with the radial array agree well with the theoretical helical Ohmic equilibrium profiles with the assumption of its toroidal rotation. The internal magnetic fields oscillate and phase of the radial field differ from those of poloidal and toroidal fields by $\pi/2$ in most of the flat-topped current phase (for ~1.0 ms); that is, absolute values of radial field fluctuations are high in the time when that of poloidal and toroidal ones are low, and vice versa, as shown in Fig. 5. Thus, the rotation seems to be quasi-stationary in the flat-topped current phase. However, this rotating picture does not necessarily agree very well with the quasi-periodic appearance of QSH defined by the edge magnetic measurements. This slight discrepancy between the internal and external magnetic field measurements may be caused by the interaction between the internally resonant dominant mode and field errors near the edge.

Another possibility of the quasi-periodic appearance of QSH or modulation of the amplitude of dominant mode is implied by the experiment and analysis in EXTRAP T2R device [19]. In recent experiments with controlled external error fields, they showed that interaction of the rotating tearing mode with external resonant magnetic perturbation causes modulation of the amplitude and phase shift of the rotating tearing mode. Experiments under well-controlled field errors are the next step necessary for further improving the quality of QSH in RELAX.

5. Conclusion

Characteristics of QSH states have been studied in a low-aspect-ratio RFP machine RELAX mainly by magnetic diagnostics. Internal profiles of radial, poloidal and toroidal magnetic fields have shown good agreement with eigenfunctions of a single helical mode. The edge magnetic fluctuation spectra are somewhat broader than what are expected from internal magnetic field profiles. In spite of these slight discrepancies, the usual measure for the QSH, the spectral index N_S lower than 2, still provides a reasonable measure for QSH state in RELAX. The QSH duration and fraction (persistence) have been improved by reduction of the poloidal resistance of flanges at poloidal gaps, mainly due to the improved toroidal symmetry of the toroidal magnetic field. QSH persistence over 30% of the flat-topped current phase has been realized with current density lower than in other RFP and without external field control, and probability of the spontaneous QSH persistence is $12.8 \pm 7.3\%$ which is higher than high-aspect-ratio EXTRAP-T2R (< 3%). It suggests the advantage of low-A configuration in attaining to the QSH.

Acknowledgments

This work is supported by a Grant-in-Aid for JSPS Fellows (21·9943), a Grant-in-Aid for Scientific Research (No. 22360390) from the Ministry of Education, Culture, Sports, Science and Technology, and partly by a NIFS collaboration program (No. NIFS07KOAH022).

[1] P. Martin *et al.*, Nucl. Fusion **43**, 1855 (2003).
[2] R. Lorenzini *et al.*, Nature Physics **5**, 570 (2009).
[3] D.F. Escande *et al.*, Phys. Rev. Lett. **85**, 3169 (2000).
[4] H. Sugimoto *et al.*, Plasma Phys. Control. Fusion **47**, 1287 (2005).
[5] T. Onchi *et al.*, Plasma Fusion Res. **3**, 005 (2008).
[6] T. Onchi *et al.*, Rev. Sci. Instrum. **81**, 073502 (2010).
[7] T. Onchi *et al.*, J. Phys. Soc. Jpn. **80**, 114501 (2011).
[8] A. Sanpei *et al.*, Plasma Fusion Res. **6**, 2406096 (2011).
[9] S. Masamune *et al.*, J. Phys. Soc. Jpn. **76**, 123501 (2007).
[10] A. Sanpei *et al.*, J. Plasma Fusion Res. SERIES **8**, 1066 (2009).
[11] A. Sanpei *et al.*, J. Phys. Soc. Jpn. **78**, 013501 (2009).
[12] R. Ikezoe *et al.*, Plasma Phys. Control. Fusion **53**, 025003 (2011).
[13] R. Ikezoe *et al.*, Plasma Fusion Res. **3**, 029 (2008).
[14] K. Oki *et al.*, J. Phys. Soc. Jpn. **77**, 075005 (2008).
[15] J.M. Finn *et al.*, Phys. Fluids B **4**, 1262 (1992).
[16] R. Paccagnella, presentation at the IEA/RFP Workshop in Madison (2000).
[17] L. Frassinetti *et al.*, Phys. Plasmas **14**, 112510 (2007).
[18] D. Bonfiglio *et al.*, Nucl. Fusion **51**, 063016 (2011).
[19] L. Frassinetti *et al.*, Nucl. Fusion **50**, 035005 (2010).